VISUAL PROPERTIES OF NEURONS ALONG THE TECTO-THALAMO-CAUDATE NUCLEUS PATHWAY

Doctoral Thesis

Zsuzsanna Paróczy

Supervisors: Prof. Dr. György Benedek

Dr. Attila Nagy

Department of Physiology, Faculty of Medicine, University of Szeged

Szeged, 2008

Table of contents

1. List of publications providing the basis of this thesis

Spatial and temporal visual properties of single neurons in the suprageniculate nucleus of the thalamus

Z Paróczy, *A Nagy, Z Márkus, WJ Waleszczyk, M Wypych, G Benedek*
Neuroscience. 2006;137(4):1397-404.
Impact factor: 3,41

Spectral receptive field properties of neurons in feline superior colliculus

*WJ Waleszczyk, A Nagy, M Wypych, A Berényi, **Z Paróczy**, G Eördegh, A Ghazaryan, G Benedek*
Exp Brain Res. 2007 Jul;181(1):87-98.
Impact factor: 2,118

Drifting grating stimulation reveals particular activation properties of visual neurons in the caudate nucleus

*A Nagy , **Z Paróczy** , Z Márkus , A Berényi , M Wypych , WJ Waleszczyk , G Benedek*
Eur J Neurosci 2008 Apr;27(7):1801-8.
Impact factor: 3,949

Multisensory responses and receptive field properties of neurons in the substantia nigra and in the caudate nucleus

*A Nagy, **Z Paróczy**, M Norita, G Benedek*
Eur J Neurosci. 2005 Jul;22(2):419-24.
Impact factor: 3,949

2. Introduction

The visual system deals with an enourmous amount of information arriving via electromagnetic waves in the range between 400 and 700 nm. Its task is to extract the relevant information continuously from this caleoidoscopic quantity of incoming light rays and initiate the mobilization of the motor system for the appropriate response in an appropriate time. The task, therefore, is the reduction of information to an amount that leads to perception of the relevant stimulus or to a simple motor response. How the visual system performs this task has been at the focus of visual research during the last 50 years.

The simplest way to extract the relevant information from the incoming optical pattern is feature detection. The extraction of elementary features makes the task of the higher centers easy. They merely have to put the pieces together into a holistic image. The task is simpler than in the case of a jigsaw puzzle since the spatial organization is determined by the retinotopic organization of the visual pathway.

Indeed, in the era of extracellular micrelectrode recordings, Barlow (1972) and Hubel and Wiesel (1977) suggested that simple cells in the visual cortex are feature detectors. We now know that a single cell cannot unambiguously tell us whether there is a feature of a particular type in the image. This is because both a non-optimal high-contrast stimulus and an optimal low-contrast stimulus will drive the cell.

Alternatively, we can think of cells in the visual cortex as filtering the image. The idea that the visual system acts as a spatial filter was initiated by the Cambridge visual research group. Campbell and Robson (1968) measured the contrast threshold for sinewave patterns and square wave patterns of the same spatial frequency. The question was raised of whether the threshold depends upon the contrast of the pattern *per se* or the contrast of the sinewave components of the pattern. It is important to know that the amplitude of the sinewave

component at the fundamental frequency of the square wave is $4/\pi$ greater than the amplitude of the square wave pattern. Campbell and Robson found that the contrast threshold of the square wave was lower than that for the sinewave of the same frequency by precisely the amount predicted by the idea that threshold for the subject depended upon the contrast of the fundamental sine wave component of the square wave rather than the contrast of the square wave pattern *per se*. These findings can be explained by the existence within the nervous system of linearly-operating independent mechanisms selectively sensitive to limited ranges of spatial frequencies. They concluded from this that the visual system acts as a spatial filter, where it is the contrast of the components and not the overall pattern that determines whether a pattern can be detected.

When a subject stares a pattern for a long time, the visual system becomes adapted. The underlying mechanism of adaptation has not been fully clarified. However, what is clear is that adaptation to a high-contrast pattern has the result of making it more difficult to see a low-contrast pattern. The question arises of whether adaptation to a single spatial frequency affects the whole of the contrast sensitivity function (CSF) or simply the sensitivity to the test frequency (Fig 1A,B). The contrast sensitivity is defined as the inverse of the contrast threshold. A plot of the sensitivity as a function of the spatial frequency is known as the CSF, which was first measured by Schade (1956). The experimental evidence that answered the previous question was presented by Blakemore and Campbell (1969), who measured the CSF before and after adaptation to a sinewave of a particular spatial frequency. They found that the contrast thresholds were elevated for only a limited range of spatial frequencies close to the adapting frequency. They concluded that the adaptation isolated a particular channel in the brain and that the CSF was the envelope of a number of overlapping spatial frequency-selective channels.

A B

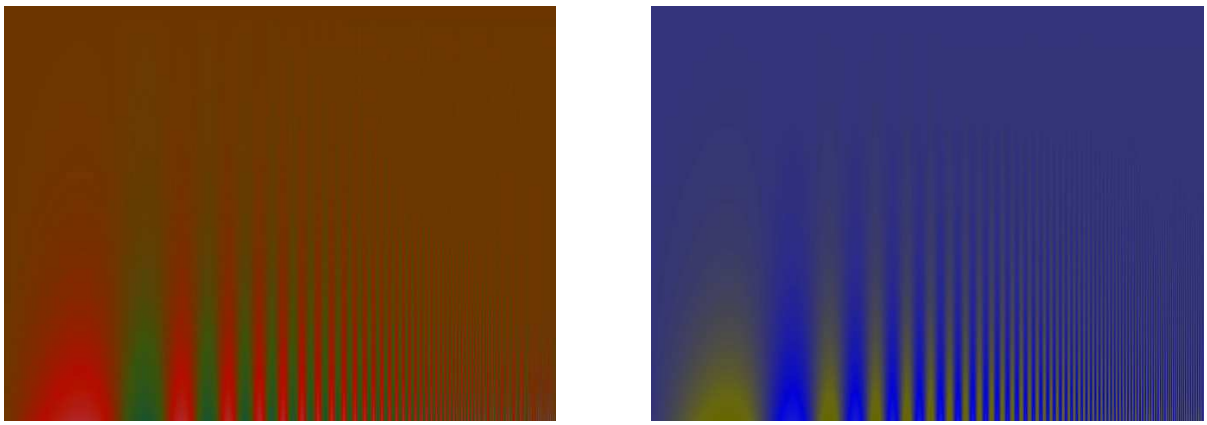

Figure 1. *Contrast sensitivity test patterns.* ***A****: Red-green isoluminant grating: the sensitivity is higher for lower spatial frequencies than in the luminance grating; and very high frequencies are somewhat less visible.* ***B****: Blue-yellow isoluminant grating: the sensitivity is higher for lower spatial frequencies than in the luminance grating; high frequencies are much less visible.*

If the visual system splits the image into separate spatial frequency bands, then interactions between channels may influence the perception. Blakemore and Sutton (1969) found that, after adaptation to a sinewave grating of a particular spatial frequency, a grating of low spatial frequency appeared to be even lower, and gratings of high spatial frequency appeared to be even higher.

An explanation of the spatial frequency shift requires a model of how activation in a range of channels gives rise to the perception of a specific spatial frequency. One possibility is that spatial frequency is encoded in terms of the distribution of activity across a population of spatial frequency-coded channels. Blakemore and Sutton (1969) suggested that adaptation to a lower spatial frequency reduces the response in that channel to the test spatial frequency and accordingly shifts the peak of the distribution away from the adapting spatial frequency**.** Another possibility (DeValois and DeValois, 1988) is that spatial frequency is encoded in terms of the relative activation of tuned channels.

Contrast adaptation is both orientation- and spatial frequency-specific (Blakemore and Campbell, 1969). An orientation-specific after-effect too may be discerned, the tilt after-effect, which is similar to the spatial frequency shift. Adaptation to a particular orientation has the effect of shifting the apparent orientation of adjacent orientations away from the adapting orientation. These results indicate that channels are tuned to both orientation and spatial frequency. Psychophysical data have established the dependence of contrast sensitivity upon the temporal frequency in humans (Robson, 1966; Tolhurst, 1973) and in cats (Pasternak, 1986, Campbell et al., 1973). On increase of the velocity of the stimulus, neither the bandpass nor the maximum of the contrast-sensitivity curve was found to decrease. The effect of notion is simply that of sliding down the spatial-frequency window toward lower spatial frequencies. Increase of the velocity of the stimulus is accompanied by a loss in sensitivity at high spatial frequencies and an increase in sensitivity at lower ones.

One way to determine the most detectable spatial pattern would be to show observers all spatial patterns and measure the sensory threshold for each. The problem with this is that in practice we could never show all the patterns that can be produced. Opticians seek the smallest letter that a subject can perceive but this gives merely a measure of acuity, and not a measure of the visibility for all patterns. There is a way to answer this question, however which depends on the Fourier decomposition of a spatial pattern.

The 18th-century French mathematician Jean Baptiste Fourier is credited with the elegant concept that any one- or two-dimensional pattern, no matter how complex, can be exactly represented by the sum of a series of sinewave components of varying frequency, amplitude, phase (position) and (for two-dimensional patterns) orientation. During the past quarter of a century, a substantial body of psychophysical and physiological evidence has amassed which strongly supports the idea that the visual system performs a Fourier-like analysis of the retinal image. The mechanisms – underlying this Fourier-like analysis are called spatial

frequency channels, whose neural embodiments are collections of receptive fields which share the property of being maximally sensitive to sinusoidal components of the visual image at particular spatial frequencies, phases and orientations.

A number of investigations of the responses of striate cortical neurons to sinewave gratings have shown that the optimal measured spatial frequency is independent of the temporal frequency at which the measurement was made (Tolhurst and Movshon, 1975; Holub et al., 1981). Such cells are generally described as having a 'separable' dependence on spatial and temporal frequencies. McLean and Palmer (1989) reported this separable dependence in the responses of A18 neurons, similar to those in the striate cortex. The CSF in cats has been shown to be dependent on temporal parameters, such that higher spatial frequencies are detected better at lower temporal frequencies (Pasternak, 1986); a similar interaction has been observed in humans (Robson, 1966; Tolhurst, 1973). The ability of the visual neurons to shift their optimal spatial frequency depending on the temporal frequency may explain the CSF of the cells.

The responses of neurons to drifting gratings of different spatial and temporal frequencies can be interpreted in terms of the dimensions and distribution of spatially and temporally summating excitatory and inhibitory components within their receptive fields (Zumbroich et al., 1988). Thus, a description of the spatiotemporal filter properties can contribute to an understanding of the role of these neurons and the cortical and subcortical brain structures in visual information processing and the connected behavioral actions.

In the visual system of mammals and vertebrates, information about the world is processed and conveyed from the retina to the brain centers by distinct, largely parallel information channels (Burke et al., 1998; Dreher et al., 1996; Livingstone and Hubel, 1988; Rowe, 1991; Stone, 1983; Stone et al., 1979). The existence of separate geniculate and extrageniculate

visual systems in the feline brain has been proved in both morphological and physiological studies (Rosenquist, 1985). The geniculostriate pathway consists of the retinal projections to the thalamic dorsal lateral geniculate nucleus (LGNd) and the subsequent projections to the primary visual cortex (A17; Hubel and Wiesel, 1962). Besides the lateral geniculate nucleus (LGN), several subcortical structures have been found that receive afferents directly from the retina (Rosenquist, 1985). One of these structures is the superior colliculus (SC), whose neurons provide the origin of the tectal ascending extrageniculo-extrastriate visual system (Fig. 2). The pathway starts from the intermediate and deep layers of the SC, its thalamic relay nucleus is in the suprageniculate nucleus (Sg) and it projects to practically the whole extent of the anterior ectosylvian sulcus (AES) and to the dorsolateral part of the caudate nucleus (CN) (Hoshino et al., 2004).

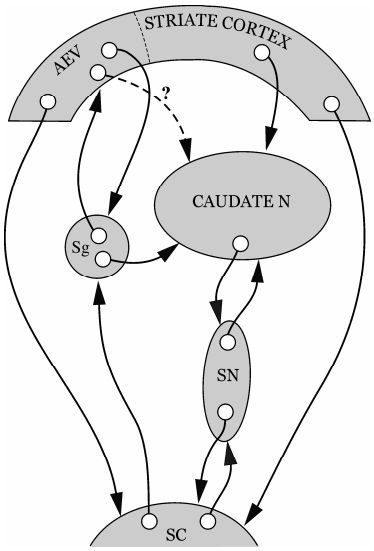

Figure 2. *Connections of extrastriatal visual cortical and subcortical structures in the feline brain. Abbreviations: AEV: anterior ectosylvian visual area, Sg: suprageniculate nucleus, SC: superior colliculus, SN: substantia nigra*

Since the tectal source of visual information toward the AEV was confirmed by morphological experiments (Harting et al., 1992), it should be noted that the responses of the neurons in both the SC and the AEV are characterized by the excitatory Y- and W-inputs from the retinal ganglion cells (Wang et al., 1998; 2001). These cells, which constitute the

entrance point of the X-, Y- and W-channels, differ not only in morphology, but also in many physiological features and are therefore postulated to play different functional roles in vision. The X-channel, characterized by relatively high spatial resolution and poor temporal resolution, is postulated to be involved in processing information relating to high acuity pattern vision (Dreher et al., 1996; Rowe, 1991; Stone 1983; Stone et al., 1979). By contrast, the spatial resolution of Y- and W-cells is much lower both in the retina (Rowe and Cox, 1993) and in LGNd (Saul and Humphrey, 1990; Sireteanu and Hoffmann, 1979; Stone, 1983; Stone et al., 1979; Sur and Sherman, 1982). The Y-channel, characterized by high temporal resolution, good responsiveness at high stimulus velocities and nonlinear spatial summation within the receptive field, appears to be involved in the processing of information concerning fast-moving stimuli (Burke et al., 1998; Dreher and Sanderson, 1973; Dreher et al., 1993; 1996). By contrast, both X- and W-cells respond optimally to stimuli moving at low velocities (Stone and Hoffmann 1972; Lee and Willshaw 1978, McIlwain 1978). Finally, the W-type retinal ganglion cells, with their heterogeneous receptive field properties and poor spatial resolution, might underlie ‘ambient’ vision, which includes the perception of visual space, some low spatial resolution pattern vision and controll of the reflex direction of the gaze (Rowe and Cox, 1993; Stone, 1983; Stone et al., 1979).

Although theoretical considerations suggest that spatial and temporal frequency sensitivity functions fully describe the responsiveness of neurons to any kind of stimuli, no study has yet been performed that involved a systematic examination of the responses of these neurons to sinusoidally modulated gratings. Since the mechanisms of visual perception depend critically upon how visually responsive neurons process and integrate spatial and temporal information, we set out to investigate and compare the responsivities of the SC, Sg and CN visual neurons to different spatial and temporal frequencies with a sinusoidally modulated luminance profile.

3. Aims of the study

The goals of our experiments were to describe the spatio-temporal spectral visual receptive field properties of neurons in the SC, the Sg and the CN of the feline brain in order to achieve a better understanding of the function of the tecto-thalamo-striatal system in visuomotor control and the connected behavioural actions.

Our concrete aims were:

- To record visual neurons in the tecto-thalamo-striatal visual system of the feline brain
- To investigate the visual receptive field properties of the neurons in the SC, the Sg and the CN
- To describe the spatial and temporal frequency preferences of the single-neurons in the SC, Sg and CN
- To investigate the spatial and temporal frequency tuning functions in the SC, Sg and CN
- To compare the spatio-temporal properties along the tecto-thalamo-striatal visual system
- To suggest the functional role of the tecto-thalamo-striatal visual system in visual information processing and the connected visuomotor actions

4. Materials and methods

4.1. Animal preparation and surgery

All procedures were carried out to minimize the number and the suffering of the animals and followed the European Communities Council Directive of 24 November 1986 (86 609 EEC) and the National Institutes of Health guidelines for the care and use of animals for experimental procedures. The experimental protocol has been accepted by the Ethical Committee for Animal Research of Albert Szent-Györgyi Medical and Pharmaceutical Center at the University of Szeged were carried out on a total of 44 adult cats of either sex ranging in weight from 2.5 to 3.5 kg. The cats were initially anesthetized with ketamine hydrochloride (30 mg/kg i.m.). The trachea and the femoral vein were cannulated and the animals were placed in a stereotaxic headholder. Wound edges and pressure points were treated generously with procaine hydrochloride (1%). The anesthesia was continued with halothane (1.6% during surgery and 0.6% during recordings). The depth of anesthesia was monitored by repeatedly monitoring the pupil size, electrocorticogram and electrocardiogram. The animals were immobilized with gallamine triethiodide (Flaxedil, 20 mg/kg i.v.). A liquid containing gallamine (8 mg/kg/h), glucose (10 mg/kg/h) and dextran (50 mg/kg/h) in Ringer's solution was infused at a rate of 3 ml/h. The end-tidal CO_2 level and the rectal temperature were monitored continuously and kept approximately constant, at 3.8-4.2% and 37-38 ^{o}C, respectively. The skull was opened with a dental drill to allow a vertical approach to the SC, Sg and the CN. The dura was covered with a 4% solution of agar dissolved in Ringer solution at 38 ^{o}C. The eye contralateral to the cortical recording was treated with phenylephrine (10%) and atropine (0.1%) and was equipped with a +2 diopter contact lens. The ipsilateral eye was covered during stimulation. A subcutaneous injection of

0.2 ml 0.1% atropine was administered preoperatively. The retinal landmarks and major retinal blood vessels were projected routinely twice daily onto a tangent screen using a fiber optic light source (Pettigrew et al., 1979). Area centralis was plotted by reference to the optic disc (14.6 deg medially and 6.5 deg below of the center of optic disc) (Bishop et al., 1962).

4.2. Recording

Electrophysiological extracellular single-cell recordings were performed by tungsten microelectrodes in the SC, the Sg and the CN of anaesthetized, immobilized artificially respirated cats. The impedance of the electrodes were ranged between 2.0 and 4.0 MOhm (AM System Inc. USA). The signal was ampilfied, visualized on an oscilloscope and monitored on an loudspeaker. First, the electrode was introduced into the LGN according to the coordinates A: 6-7, L: 8-10 and depth: 12-16 mm. The exact position of the electrode tip was determined according to a comparison of the actual receptive field position with LGN atlas by Sanderson (1971). This correction enabled an accurate aiming of the SC, the Sg and the CN.

Neuronal activities were recorded by a computer and stored for further analysis as peristimulus time histograms (PSTHs). Vertical penetrations were performed between the Horsley-Clarke co-ordinates anterior 6 to posterior 1, lateral 0-6 in the stereotaxic depths in the interval 15-17 to record SC; anterior 4.5-6.5, lateral: 4-6.5 in the stereotaxic depths in the interval 16-18 to record Sg; anterior 12-17 and lateral 4-6.5 in the stereotaxic depths in the interval 12-19 to record CN neurons.

4.3. Visual stimulation and data analysis

Directional tuning and spatio-temporal frequency characteristic of each unit were

tested with drifting sinewave gratings displayed on the monitor (refresh rate: 85 Hz) positioned at a distance of 42.9 cm from the cat's eye. The diameter of the stimulation screen was 22.5 cm, and the cat therefore saw it in 30 deg The contrast of the grating was held constant at 96% (Michelson contrast= $(L_{max} - L_{min})/(L_{max} + L_{min})$, where L_{max} and L_{min} are maximum and minimum luminance of the spatial sinusoid, respectively). The mean luminance of the screen was 23 cd/m^2.

For study of the spatio-temporal characteristics of the cells, the sinusoidal gratings were moved along 4 different axes in 8 different directions (0-315 deg at 45 deg increments) to find the optimal moving direction of each unit. The optimal direction of each unit was used further to describe its spatial and temporal tuning characteristics. The tested spatial frequencies ranged from 0.025 to 0.95 cycle/deg (c/deg) and the temporal frequencies from 0.07 to 41.08 cycles/second (c/sec, Hz). Stimuli were presented in a pseudo-random order in a series consisting of 8 spatio-temporal frequency combinations of moving gratings. Each spatio-temporal frequency combination was presented at least 12 times. The interstimulus interval was consistently 1 s. Individual action potentials were distinguished with the help of a spike-separator system (SPS-8701, Australia). The number and temporal distribution of the action potentials recorded during stimulation were stored as peristimulus time histograms (PSTHs) and analysed by computer. The duration of the prestimulus period (a stationary sinusoidal grating was shown) was 1000 ms, as was the peristimulus time (a drifting sinusoidal grating was shown). The net discharge rate of a neuron was calculated as the difference between the mean firing rates of the cell obtained during stimulus movement and the background activity corresponding to the mean activity during the 200 ms preceding movement in the prestimulus interval.

To estimate the extent of direction selectivity, a direction selectivity index (*DI*) similar to that proposed by Dreher et al. (1993) was calculated by using the formula:

$$DI=100\times(R_p-R_{np})/R_{p,}$$

where R_p and R_{np} are the net discharge rates in the preferred and non-preferred (opposite) directions, respectively.

4.4. Histological control of the recording tracks

At the end of the experiments, the animals were deeply anaesthetized with sodium pentobarbital (200 mg/kg i.v.) and transcardially perfused with 0.9% saline in 0.1 M sodium phosphate buffer (pH 7.4), followed by a mixed solution of 4.0% paraformaldehyde in 0.1 M PBS with 4% sucrose added. The brains were removed and cut into coronal sections of 50 µm, and the sections were stained with neutral red. Electrolytic lesions marked the locations of successful electrode penetrations. The neurons that were used in this study were located in the SC or in the Sg or in the CN.

5. Results

5.1. Visual receptive field properties of single neurons in the superior colliculus (SC)

Altogether 99 visually active single neurons were recorded in the intermediate layers of the SC (stratum griseum intermedium and stratum album intermedium). Some of these SC neurons were multisensory, they responded also to auditory and/or somatosensory modalities tested. We determined the location and size of the neurons' receptive fields with the help of a hand-held lamp, by listening to the increase of the neuronal response to visual stimulation. After converting our calculated Cartesian co-ordinates to polar co-ordinates according to the formulae published by Bishop et al. (1962), we determined the size of the receptive field in degree^2. The mean size of the receptive fields in the intermediate layers of the SC was 1890.69±1005,89 degree^2 (N=99, Range: 310.1-4643.9).

5.2. Direction sensitivity and tuning function of the collicular neurons

The preference for the different directions were common among the SC neurons (Fig.3A). The direction sensitivity and tuning function of the SC cells were determined on the basis of their responses to the drifting sinewave gratings moving in eight different directions (four different axes of movement) with the optimal spatial and temporal frequencies of each unit. The direction sensitivity of the cells was calculated by using *DI* (Dreher et al., 1993). A majority of the SC neurons (41/99, 41%) exhibited *DI*s of <50%, and these units were therefore classified as non-direction-sensitive cells. However, 35 of the 99 SC neurons (36%) had *DI*s >70% and accordingly were classified as direction-selective,

while 23 SC neurons (23 %) had *DI*s between 50 and 70% and were direction-sensitive (Fig. 3B).

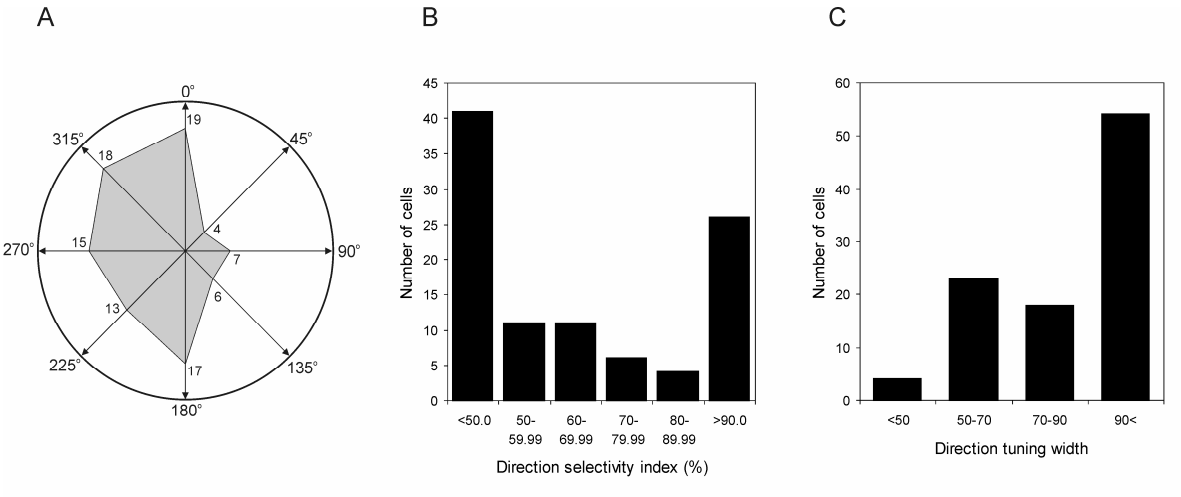

Figure 3. ***A:*** *Distribution of the prefered directions of the 99 single units recorded in SC. The number of single neurons that showed preference for directions indicated by the arrows.* ***B:*** *A large majority of the recorded collicular neurons are non-direction selective, with low DIs of <50%.* ***C:*** *Distribution of the direction tuning widths. A majority of the SC neurons exhibited broad direction tuning, characterized by a tuning width of ≥ 90 deg.*

The direction tuning of the visually active neurons was characterized by the tuning width, which was defined as the range of directions over which the magnitude of the responses was at least half of the maximum one. Most of the collicular cells (57/99; 58%) exhibited broad direction tuning, characterized by a tuning width of 90 deg or more (Fig. 3C), while a smaller proportion of the neurons (42/99; 42%) were narrowly tuned, characterized by a tuning width of less than 90 deg. The average of the direction tuning width was 116 deg (N=99, Range:47-347 deg, SD: ±65 deg).

5.3. Spatio-temporal frequency tuning function in the SC

The spatial frequency tuning function of the SC neurons was determined on the basis of their responses to drifting sinewave gratings moving in the optimal direction with optimal

temporal frequency. Figure 4A demonstrates the responses of a typical collicular, visually active cell to different spatial frequencies.

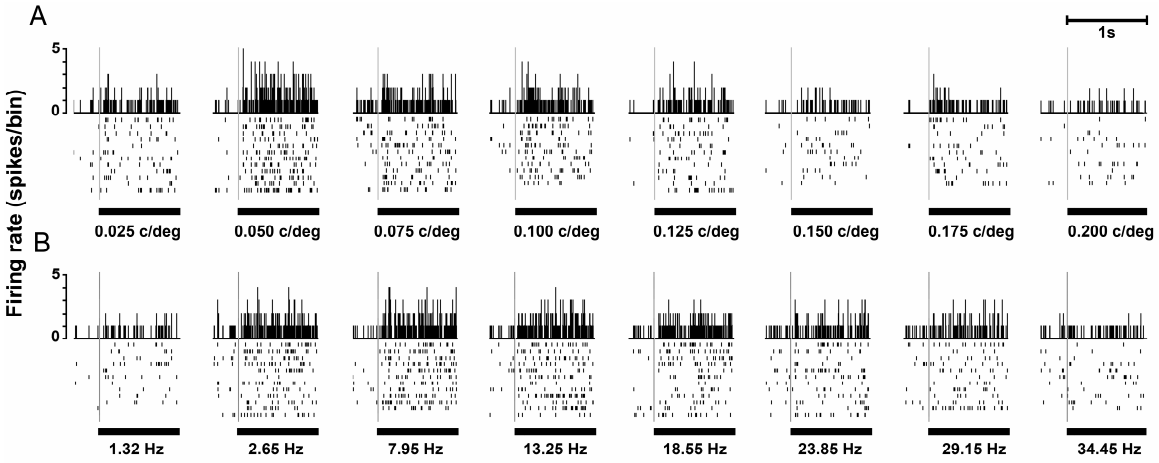

Figure 4. *PSTHs and raster plots of a typical SC single neuron responding to sinusoidally modulated drifting gratings with different spatial and temporal frequencies. Under the PSTHs the corresponding spatial and temporal frequencies of the sinewave gratings are displayed. The ordinate denotes the discharge rate in Hz. The thick black lines under the PSTHs indicate the duration of the stimulus movement for 1000 ms (peristimulus time) .* ***A****: Responses of the SC neuron to eight different spatial frequencies. The gratings were moved in the optimal direction at the optimal temporal frequency of this unit.* ***B****: Responses of the SC neuron to eight different temporal frequencies. The gratings were moved in the optimal direction at the optimal spatial frequency of this unit.*

The collicular neurons in the intermediate layers of the SC responded optimally to low spatial frequencies (Fig.5D). The mean optimal spatial frequency in the intermediate layers was 0.06 ±0.02 c/deg (N=99, Range: 0.025-0.25 c/deg).

Over a half of the neurons in the intermediate (53/99; 54%) layers of the SC displayed spatial low-pass tuning and there was either no or only a slight attenuation of the response at low spatial frequencies (Fig. 5A). The remainder of the neurons (24/99; 24%) exhibited band-pass spatial frequency tuning (Fig. 5B). In these neurons we could find an attenuation of the response to at least half the height of the maximum. We detected 10 (10/99; 10%) neurons, which displayed broad-band spatial frequency tuning characteristics (Fig. 5C) and

only a single (1/99; 1%) neuron with high-pass spatial frequency tuning. In case of 11 cells (11/99; 11%) we couldn't find any clear spatial frequency tuning.

For neurons with spatial band-pass characteristics, the mean spatial frequency bandwidth was 1.06±0.56 octaves (N=24, Range: 0.1-2.18 octaves, Fig. 5E).The spatial resolution, characterized by the spatial high-frequency cut-off value, was determined in 51 neurons in the intermediate layers of the SC (Fig. 5F). The mean spatial resolution of these neurons was 0.17±0.05 c/deg (N=51, Range: 0.06-0.37 c/deg).

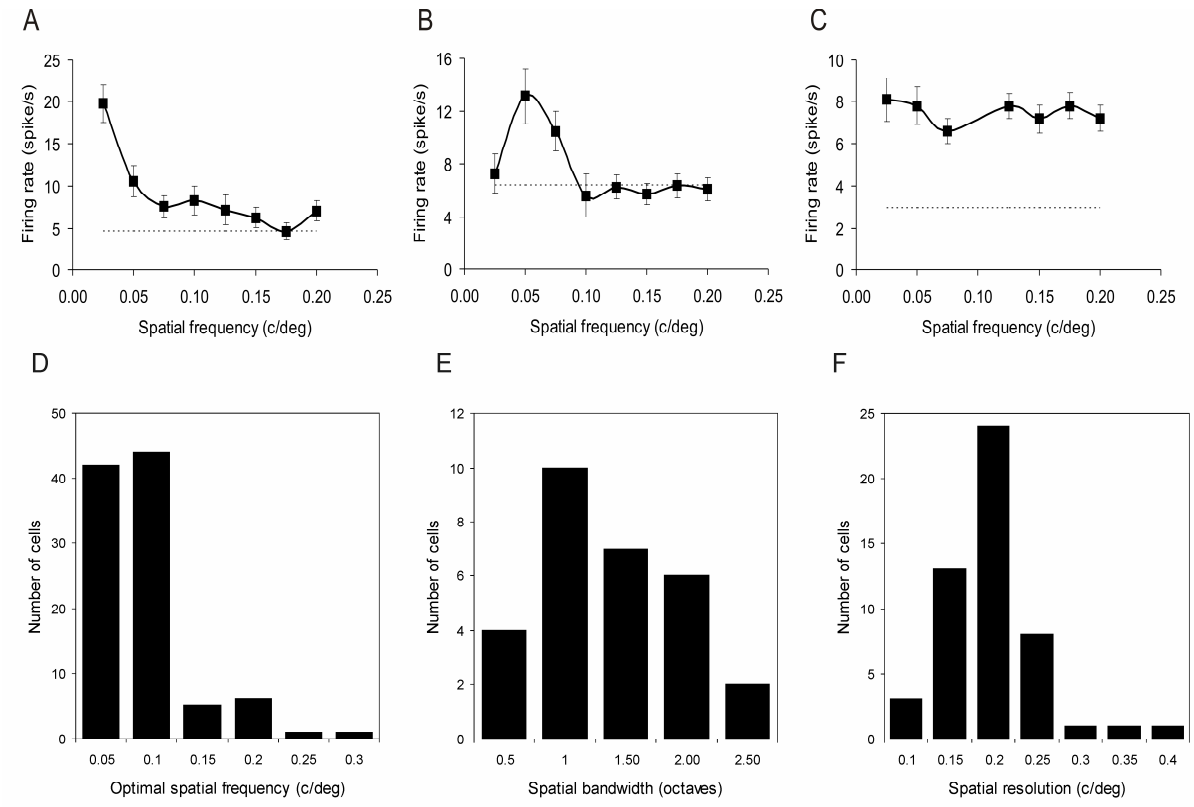

Figure 5*. Visual spatial frequency properties of the SC neurons.* ***A-C****: Examples of spatial frequency tuning functions of the SC. Each point (square symbol) corresponds to the mean firing rate for a particular spatial frequency. Each error bar corresponds to the standard error of the mean. The dashed lines indicate the level of the spontaneous activity.* ***D****: Distribution of optimal spatial frequencies estimated from the spatial frequency tuning functions. Note that all cells responded optimally to extremely low spatial frequencies.* ***E****: Distribution of spatial bandwidths (full-width at half-height). Most of the band-pass units were narrowly tuned to spatial frequencies* ***F****: Distribution of the spatial resolutions.*

The neurons of the SC intermediate layer preferred the higher temporal frequencies (Fig. 6E) with a mean optimal temporal frequency of 9.06±5.49 Hz (N=99, Range: 1.71-31.93 Hz). Almost one half (48/99; 49%) of the neurons exhibited temporal band-pass frequency tuning (Fig. 6A). In the intermediate layers of the SC 16 neurons (16/99; 16%) displayed high-pass (Fig. 6B) while 17 neurons (17/99; 17%) displayed low-pass temporal frequency tuning (Fig. 6C) . We also detected 9 neurons (9/99; 9%), which exhibited temporal broad-band tuning characteristics (Fig. 6D). In case of 9 intermediate layer neurons (9/99; 9%) we couldn't find a clear temporal frequency tuning.

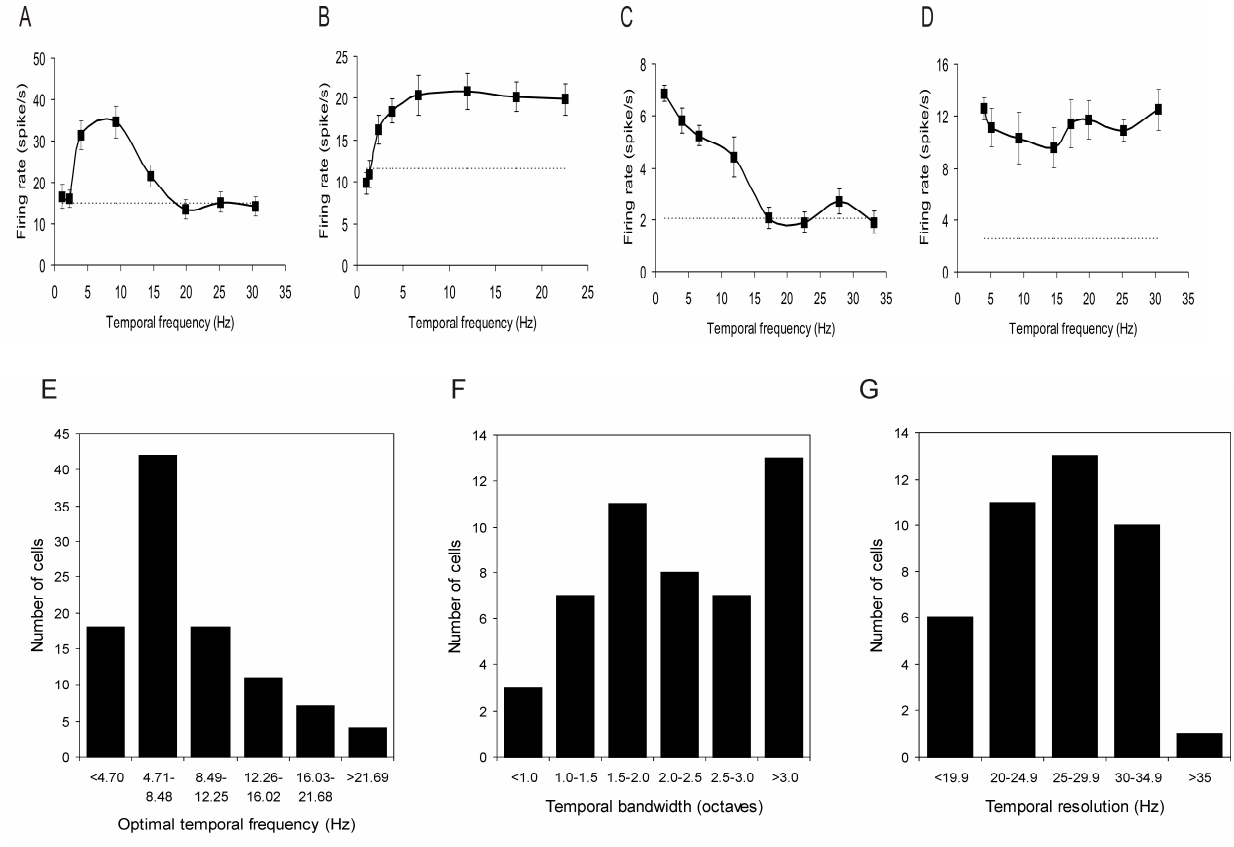

Figure 6. *Visual temporal frequency properties of the SC neurons.* ***A-D:*** *Temporal tuning curve examples for the SC neurons* ***E****: Distribution of optimal temporal frequencies of cells estimated from the temporal frequency tuning functions.* ***F****: Distribution of temporal bandwidths.* ***G****: Distribution of the temporal resolutions.*

The mean temporal high-frequency cut-off value was 22.2±10.56 Hz (N=47, Range 4.8–38.0 Hz) in the intermediate layer neurons (Fig. 6F). For neurons with temporal band-pass characteristics, the mean temporal frequency bandwidth was 2.32±0.97 octaves (N=48, Range 0.25-4.29 octaves) (Fig. 6G).

5.4. Visual receptive field properties of single neurons in the suprageniculate nucleus (Sg)

Altogether 105 visually active single-units were recorded in the Sg. The visual responses and the receptive field properties of these visually responsive suprageniculate neurons were analyzed in details. Subjective estimation of the extents of the visual receptive fields were performed by listening to the neuronal responses to the movements of a light spot generated by a handheld lamp. Our subjective estimation indicated in all cases that the visual receptive fields were extremely large (consistently larger than 6000 deg^2): they covered a major part of the contralateral hemifield and extended deep into the ipsilateral one, yielding a receptive field that overlapped almost totally with the visual field of the right eye. The receptive fields consistently included the area centralis. No signs of retinotopical organization were observed within the Sg of the posterior thalamus.

5.5. Direction selectivity and direction tuning function of the suprageniculate neurons

Using the drifting sinewave gratings moving in eight different directions with the optimal spatial and temporal frequencies, the direction sensitivity and the direction tuning function of the Sg neurons were determined. The preference for the different directions was common among the Sg neurons (Fig.7A). Sixty-seven of the 105 Sg units (67/105, 64 %) exhibited DIs higher than 70%, and thus were strongly direction-sensitive. For 11 of these 67

direction-selective single units, even inhibition of the spontaneous activity was detected (in the opposite direction). Twenty-one (21/105, 20%) Sg neurons had a DI in the interval of 50-70%, i.e. they were direction-sensitive. The remaining 17 cells (17/105, 16%) furnished DIs of <50% and were classified as non direction-sensitive (Fig. 7B).

The majority of the Sg cells (83/105, 79%) exhibited broad direction tuning, characterized by a tuning width of 90 deg or more, while a smaller proportion of the neurons (22/105, 21%) were narrowly tuned, characterized by a tuning width of less than 90 deg (Fig. 7C). The average of the direction tuning width was 180 deg (N=105, Range: 43-315 deg, SD: ±106 deg).

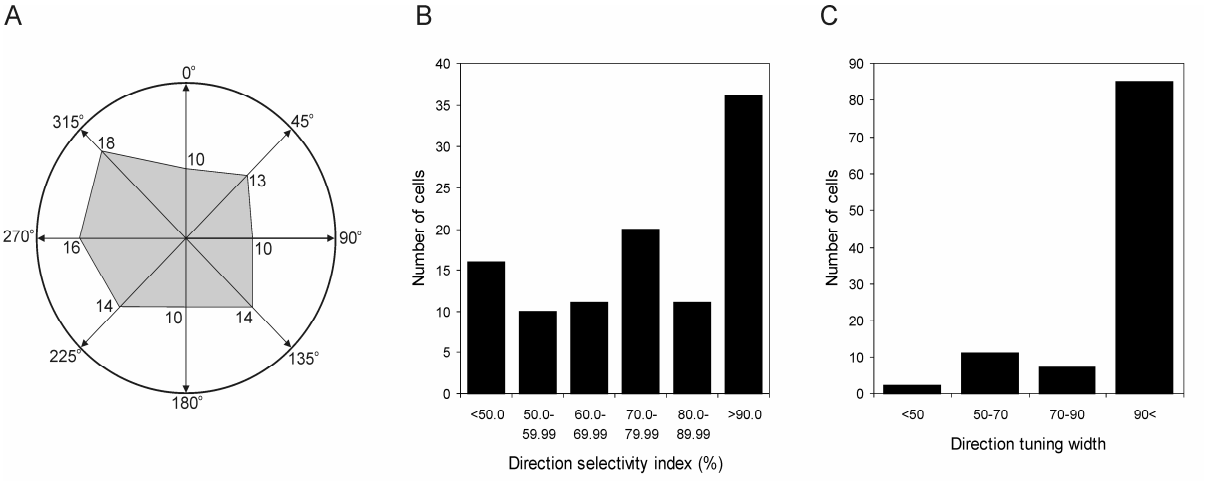

Figure 7. *The number of single Sg neurons that showed a preference for drifting directions indicated by arrows (**A**). The stimuli were high-contrast (96%) sinewave gratings with optimal spatial and temporal frequencies of each unit, drifting in 8 different directions from 0 deg to 315 deg at increments of 45 deg. The large majority of the Sg cells were direction-selective, with high direction selectivity indices (DIs) of >70% (**B**). Large majority of the recorded Sg units exhibited broad direction tuning, characterized by a tuning width of ≥ 90 deg (**C**).*

5.6. Spatio-temporal frequency tuning function of the Sg neurons

The spatial frequency tuning function of the Sg neurons was determined on the basis of their responses to drifting sinewave gratings moving in the optimal direction with the

optimal temporal frequency. All of the Sg cells, similarly to the neuron presented on Figure 8A displayed vigorous responses to low spatial frequencies.

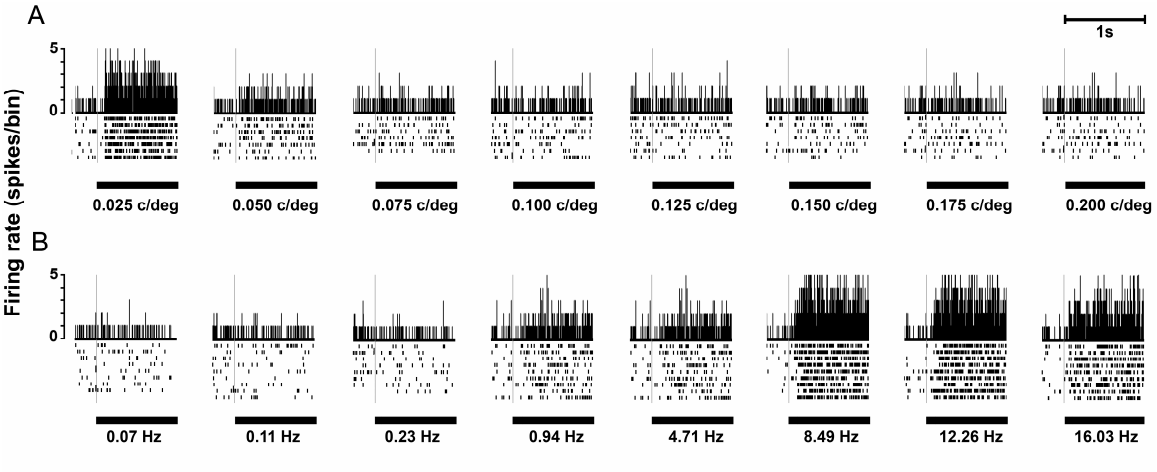

Figure 8. *PSTHs and raster plots of a Sg cell responding to drifting gratings with different spatial (**A**) and temporal frequencies (**B**). Under the PSTHs, the corresponding spatial and temporal frequencies of the sinusoidally modulated gratings are displayed.*

A maximal response could not be recorded for any of them at spatial frequencies above 0.2 c/deg. The mean optimal spatial frequency of the Sg units was 0.05 c/deg (N=105, Range: 0.02-0.2 c/deg, SD: ±0.04 c/deg) (Fig. 9D). The spatial high-frequency cut-off, regarded as a measure of the spatial resolution of the Sg neurons, was also very low (Fig. 9F)**,** with a mean of 0.1 c/deg (N=105, Range: 0.04-0.45 c/deg, SD: ±0.08 c/deg).

One-third of the units exhibited band-pass tuning characteristics (41/105, 39%); these cells had a clear optimal spatial frequency, above and below which the discharge rate was lower (Fig. 9A). The remaining two-thirds of the Sg neurons (64/105, 61%) displayed low-pass spatial tuning characteristics under the present stimulating conditions, with no attenuation of the response for the low spatial frequencies (Fig. 9B,C)**.**

The spatial bandwidths of the 41 band-pass Sg units were analyzed (Fig. 9E). The spatial bandwidth was measured at the half-height of the spatial frequency-tuning curve. This indicates the spatial selectivity of the neurons. The Sg units were very narrowly tuned to

spatial frequencies, and accordingly can serve as very good spatial filters. Half of the supragenicular units exhibited a spatial bandwidth under one octave (22/41, 54%). The mean spatial bandwidth of the band-pass tuned Sg neurons was 1.07 octaves (N=41, Range: 0.11-2.81 octaves, SD: ± 0.69 octaves).

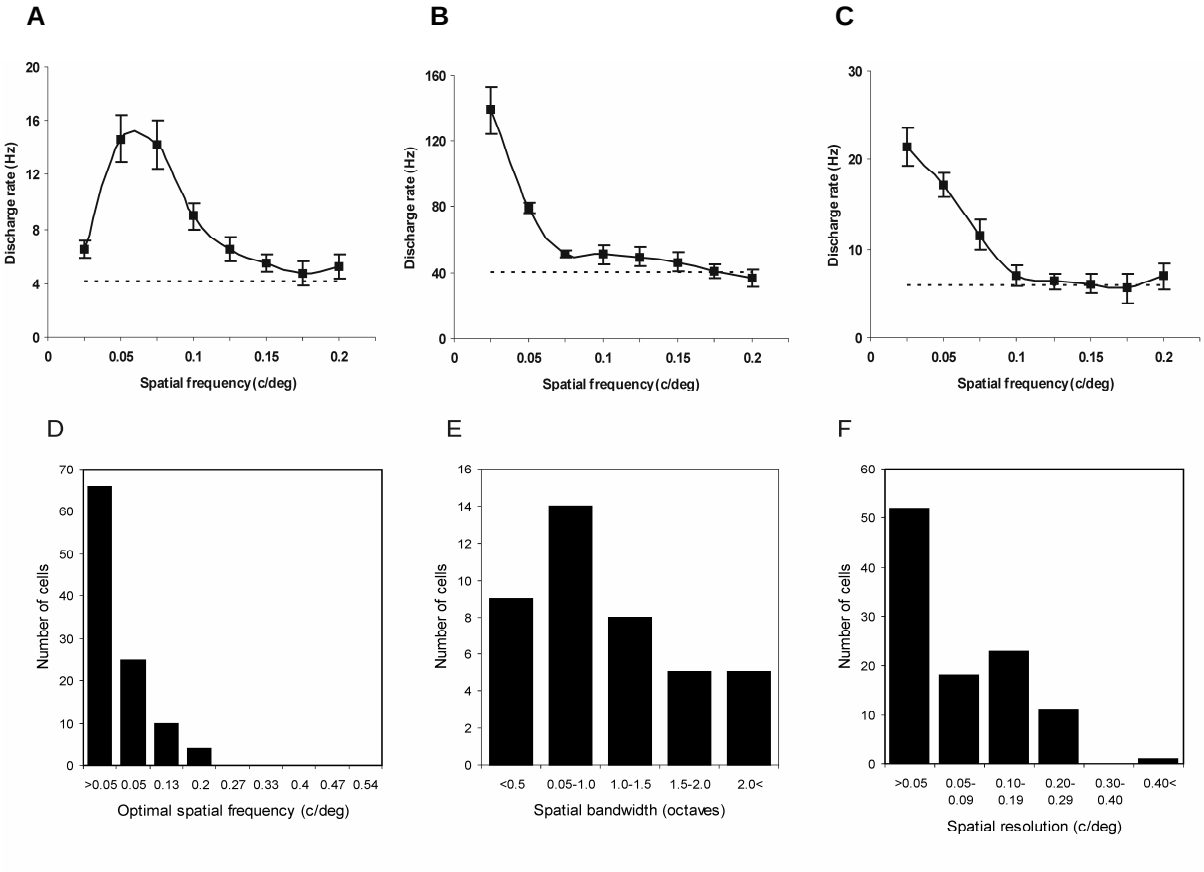

Figure 9. *Spatial visual properties of the Sg neurons.* ***A-C****: Examples of spatial frequency tuning functions in the Sg. The cell in A shows band-pass tuning characteristics, while the cells in B and C are low-pass tuned.* ***D****: Distribution of the optimal spatial frequencies estimated from the spatial frequency tuning functions.* ***E****: Distribution of the spatial bandwidths (full-width at half-height). Most of the band-pass units are extremely narrowly tuned to spatial frequencies.* ***F****: Distribution of the spatial resolution. The Sg units consistently had a very low spatial high-frequency cut-off.*

As the PSTHs of a typical visually active Sg neuron show on Figure 8B–, most of the Sg cells displayed responses to high temporal frequencies. Three kinds of temporal tuning functions were apparent under the present stimulating conditions: high-pass (29/105, 28%), band-pass (73/105, 70%) and low-pass (3/105, 2%). High-pass cells responded optimally to

the highest temporal frequency tested (Fig.10B). Low-pass cells exhibited the maximal response to the lowest temporal frequency tested; higher temporal frequencies resulted in weaker responses (Fig.10C). Overall, a large majority of the units responded optimally to high temporal frequencies, with a mean of 8.53 Hz (N=105, range: 0.07-26.41 Hz, SD: ±4.43 Hz), although we also observed cells with preferences for all examined temporal frequencies (Fig. 10D). The temporal high-frequency cut-off of the Sg units was also high. The mean temporal resolution was 15.0 Hz (*N*=105, SD: ±8.1 Hz, Range: 4.15-26.41 Hz; Fig. 10F). The temporal bandwidth, defined as the range of temporal frequencies over which the responses were at least half the maximal one, was determined for 73 band-pass units (Fig. 10A). This indicates the temporal selectivity of the cell. The cells were narrowly tuned to temporal frequencies. The mean temporal bandwidth was 1.66 octaves (N=73, Range: 0.03-7.91 octaves, SD: ±1.37 octaves) (Fig. 10E).

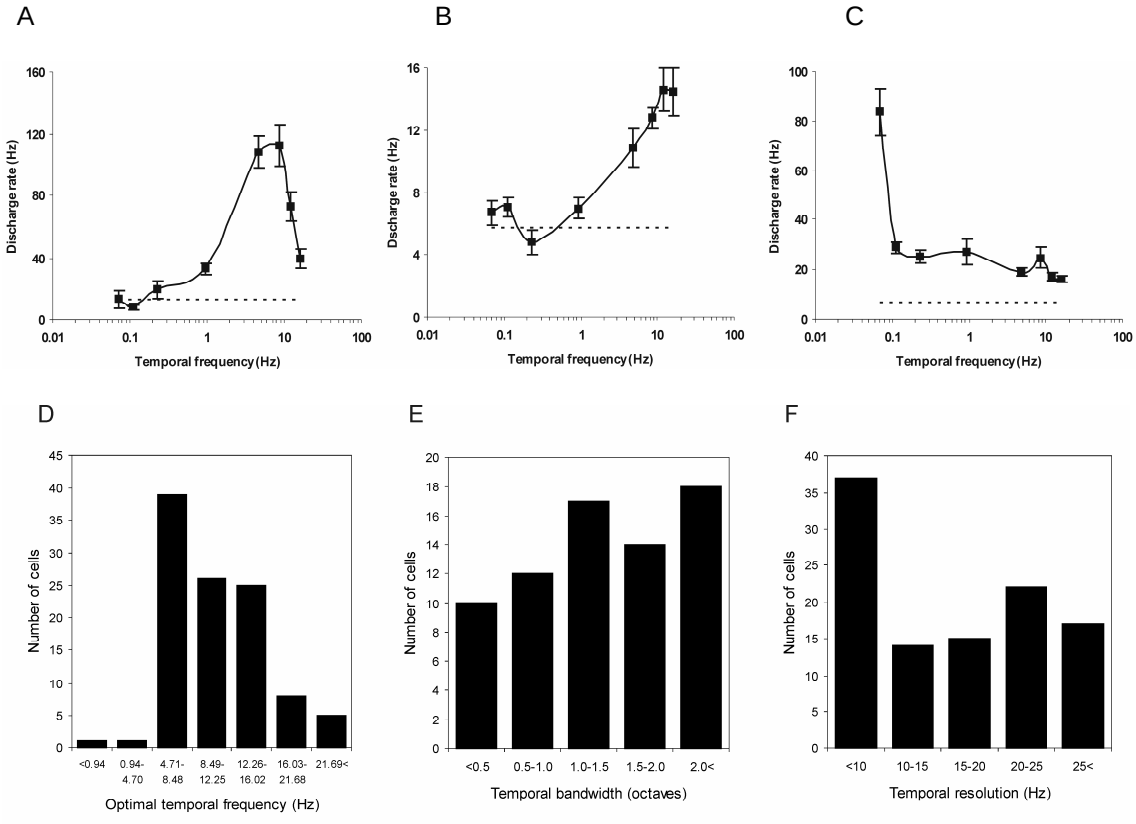

Figure 10. *Temporal visual properties of the Sg neurons.* ***A-C****: Examples of temporal frequency tuning functions in the Sg. The cell in* ***A*** *exhibited a temporal band-pass tuning function, the neuron in* ***B*** *a temporal*

*high-pass tuning function, the unit in **C** a temporal low-pass tuning function. **D**: Distribution of the optimal temporal frequencies of the cells, estimated from the temporal frequency tuning functions. The large majority of the Sg cells responded optimally to high temporal frequencies. **E**: Distribution of the temporal bandwidths (full-width at half-height). The majority of the cells displayed a relatively narrow temporal tuning.* **F**:*Distribution of the temporal resolution. The Sg units consistently had a high temporal high-frequency cut-off.*

5.7. Visual receptive field properties of single neurons in the caudate nucleus (CN)

Similarly to earlier findings, our subjective estimation of the extents of the visual receptive fields by listening to the neuronal responses to the movements of a light spot generated by a hand-held lamp demonstrated that the visual receptive fields of the registered 101 CN units were extremely large: they covered a major part of the contralateral hemifield and extended deep into the ipsilateral hemifield, yielding a receptive field that overlapped almost totally with the visual field of the contralateral eye. No signs of retinotopical organization were observed within the visually active part of the caudate body (Pouderoux and Freton, 1979; Nagy et al., 2003b, 2005b).

5.8. Direction selectivity and tuning function of the caudate neurons

The direction sensitivity and tuning functions of the CN neurons were determined on the basis of their responses to the drifting sinewave gratings moving in 8 different directions with their optimal spatial and temporal frequencies. The preferred directions varied considerably in the cells recorded. A particular direction of the movement produced a maximal response in some cells, while the remainder of the cells had preferences for other sites (Fig. 11A).

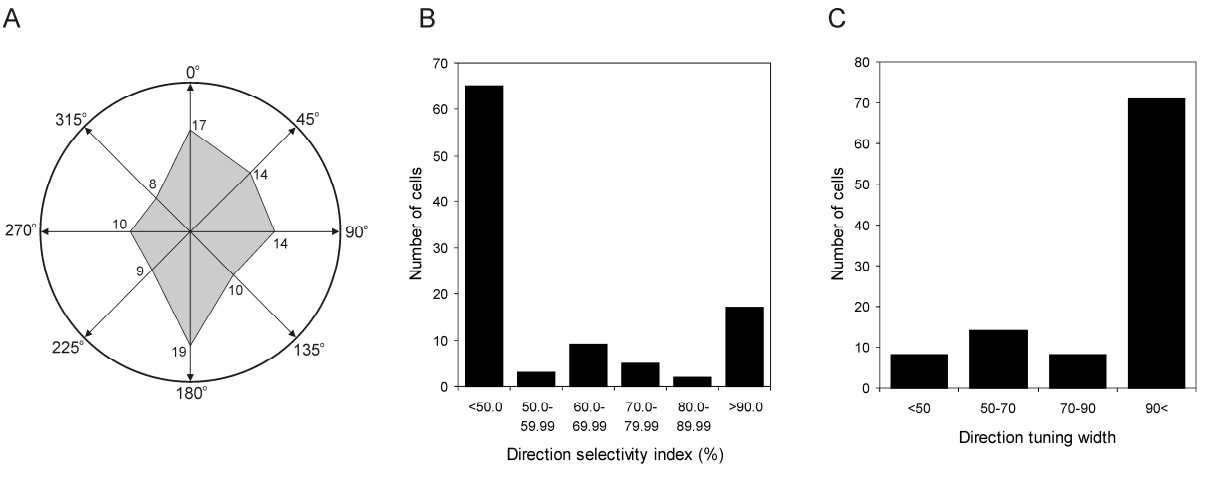

Figure 11. *Direction sensitivity and tuning function of the CN neurons.* ***A****: The number of single CN neurons that showed a preference for drifting grating directions indicated by the arrows.* ***B****: Distribution of the direction selectivity indices.* ***C****: Distribution of the direction tuning widths. A majority of the CN neurons were not direction-sensitive, with DIs of < 50% and exhibited broad direction tuning, characterized by a tuning width of ≥ 90 deg.*

A majority of the CN neurons (63/101, 62%) exhibited *DI*s of <50%, and these units were therefore classified as non-direction-sensitive cells. However, 26 of the 101 CN neurons (26%) had *DI*s >70% and were classified accordingly as direction-selective, while 12 CN neurons (12 %) had *DI*s between 50 and 70% and were direction-sensitive (Fig. 11B). A majority of the CN neurons (72/101; 71%) exhibited broad directional tuning characterized by a tuning width of ≥90 deg. In contrast, the remainder of the investigated neurons (29/101; 29%) were characterized as narrowly tuned cells with a tuning width of <90 deg (Fig. 11C). The average direction tuning width was 182 deg (*N*=101; SD: ±121.88 deg, Range: 45-360 deg).

5.9. Spatio-temporal- frequency tuning function in the CN

The spatial frequency tuning function of the CN neurons was determined on the basis of their responses to sinusoidally modulated drifting gratings moving in the optimal direction

with the optimal temporal frequency. Figure 12A demonstrates the responses of a CN cell to different spatial frequencies. Similarly to this neuron, all of the investigated CN neurons displayed strong responses to very low spatial frequencies.

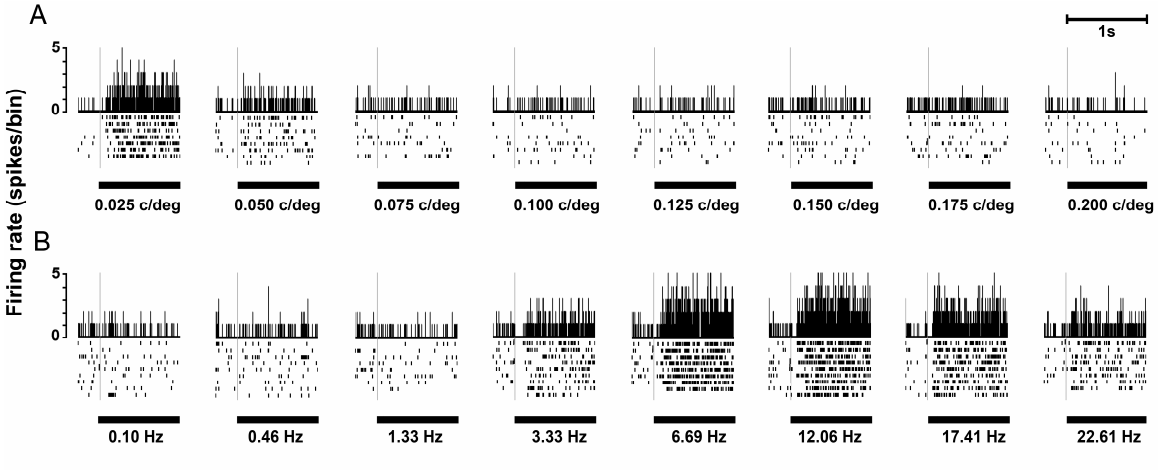

Figure 12. *PSTHs and raster plots of a typical CN single neuron responding to drifting sinewave gratings with different spatial and temporal frequencies. (**A**) Responses of a CN neuron to eight different spatial frequencies. The gratings were moved in the optimal direction at the optimal temporal frequency (12.06 Hz) of this unit. (**B**) Responses of a CN neuron to eight different temporal frequencies. The gratings were moved in the optimal direction at the optimal spatial frequency (0.025 c/deg) of this unit.*

The mean optimal spatial frequency of the CN neurons was 0.05 c/deg (*N*=89, SD: ±0.03 c/deg, range: 0.025-0.18 c/deg; Fig. 13C). The mean optimal spatial frequency may be overestimated since for 42 neurons the optimal spatial frequency was the lowest spatial frequency (0.025 c/deg) tested. The spatial resolution could be calculated for 42 CN units. In this CN neuronal population, the spatial high-frequency cut-off was consistently very low, with a mean of 0.1 c/deg (*N*=42, SD: ±0.05 c/deg, Range: 0.039-0.20 c/deg). In contrast with this finding, the responses of the remainding 47 CN neurons were slightly higher than one-tenth of the maximum of the highest spatial frequency tested (Fig. 13E); the spatial resolution for these cells was therefore >0.4 c/deg.

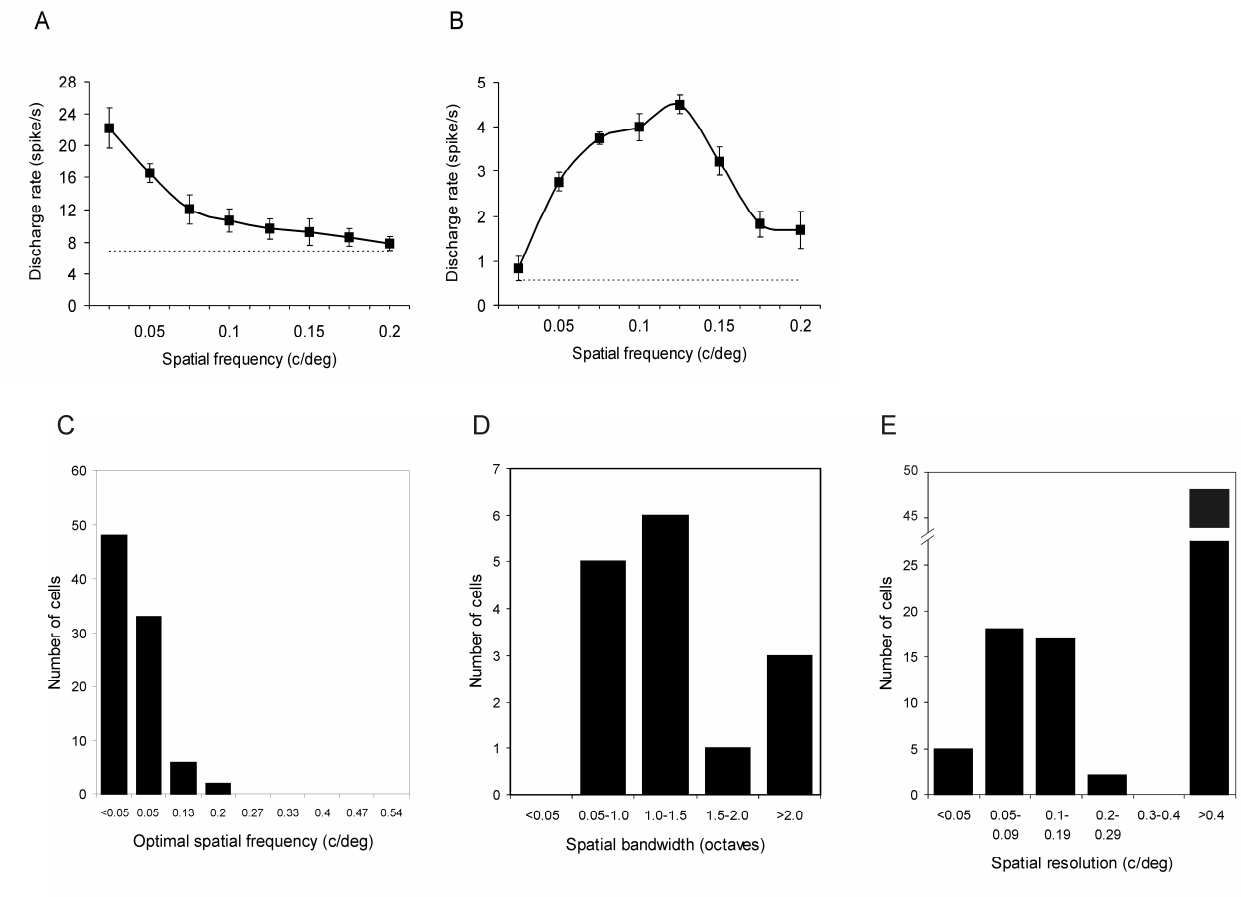

Figure 13. *Visual spatial frequency properties of the CN neurons.* ***A, B****: Examples for a low-pass and for a band-pass tuned CN neuron.* ***C****: Distribution of the optimal spatial frequencies of cells estimated from the spatial frequency tuning function. The large majority of the CN cells responded optimally to low spatial frequencies.* ***D****: Distribution of the spatial bandwidths (full-width at half-height). Most of the band-pass units were narrowly tuned to spatial frequencies.* ***E****: Distribution of the spatial resolution. The CN units consistently had a very low spatial high-frequency cut-off.*

More than half of the investigated CN neurons (55/89, 62%) displayed spatial low-pass tuning characteristics under the present stimulating conditions, with no attenuation of the response for the lowest spatial frequencies (Fig. 13A). Fifteen units (17%) exhibited band-pass spatial frequency tuning (Fig. 13B). The spatial bandwidths measured at half-height of the spatial frequency-tuning curve of the 15 band-pass CN units were analyzed (Fig. 13D). The CN units were narrowly tuned to spatial frequencies, and accordingly can serve as good spatial filters. The mean spatial bandwidth of the band-pass-tuned CN neurons was 1.31 octaves (*N*=15, SD: ± 0.76 octaves, Range: 0.37-3.0 octaves,). Another 15 of the

investigated CN units (17%) were spatial broad-band neurons that responded at almost the same level for all spatial frequencies tested. In case of 4 cells (4/89; 4%) we could not find any clear spatial frequency tuning.

All of the investigated CN units responded optimally to high temporal frequencies (Fig.14D). The mean optimal temporal frequency of the CN neurons was high: 10.6 Hz (*N*=89, SD: ±4.8 Hz, Range: 4.6-27.6 Hz). The temporal high-frequency cut-off of the CN units was also very high. The mean temporal resolution could be calculated for 31 CN neurons: it was 20.6 Hz (*N*=31, SD: ±5.6 Hz, Range: 6.3-34.1 Hz; Fig. 14F). The remaining 58 CN units still showed at least a slight response (higher than one-tenth of the maximal response) for the highest temporal frequency tested.

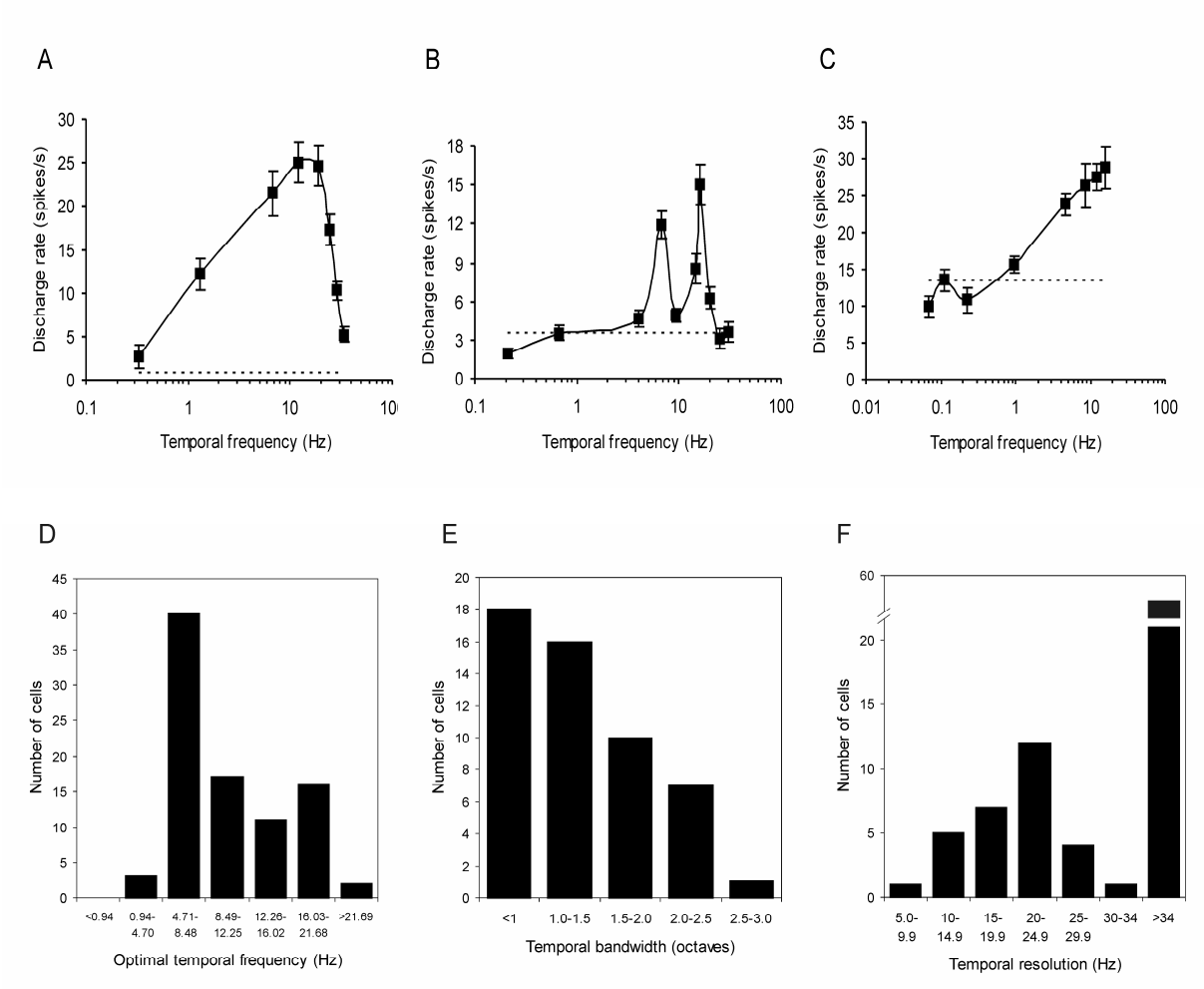

Figure 14. *Visual temporal frequency properties of the CN neurons.* ***A-C****: Examples of temporal frequency tuning functions in the caudate nucleus.* ***A****: Temporal tuning curve of a band-pass neuron.* ***B****: Tuning curve of a*

neuron tuned to two temporal frequencies. ***C****: Tuning curve of a temporal high-pass CN neuron.* ***D****: Distribution of optimal temporal frequencies of cells estimated from the temporal frequency tuning functions. The large majority of the CN cells responded optimally to high temporal frequencies.* ***E****: Distribution of the temporal bandwidths (full-width at half-height). The majority of the cells displayed a relatively narrow temporal tuning.* ***F****: Distribution of the temporal resolution. The CN units consistently had a very high temporal high-frequency cut-off.*

Fifty-five of the 89 neurons (62%) were classified as temporal band-pass cells (Fig. 14A). The band-pass CN neurons were narrowly tuned to temporal frequencies with a mean temporal bandwidth of 1.38 octaves (*N*=55, SD: ±1.0 octave, Range: 0.09-5.36 octaves; Fig. 14F). Fourteen CN neurons (16%) exhibited double temporal frequency tuning with clearly two optimal frequencies in the higher temporal frequency domain (Fig 14B). Six CN units (7%) elicited temporal high-pass tuning (Fig. 14C) and another 3 (3%) were temporal broad-band neurons. None of the CN units exhibited low-pass temporal frequency tuning. The temporal frequency tuning characteristic of 11 caudate neurons (11/89, 12%) could not be determined.

6. Discussion

Our results furnish new data concerning the representation of the visual environment in the feline extrageniculate visual system. Earlier electrophysiological studies described the responsivity of the SC (Waleszczyk et al., 1999, 2007; Dec et al., 2001; Hashemi-Nezhad et al., 2003; Stein and Meredith, 1991; Mendola and Payne, 1993), the CN (Hikosaka et al., 1989; Nagy et al., 2005b, 2003b) and the Sg visual neurons (Benedek et al., 1996; 1997) to simple geometric forms, i.e. moving spots and bars. Despite plenty of studies focusing on visual receptive field organization and properties of the neurons within the extrageniculate visual system, we have very scarce information concerning the responsiveness of these neurons to extended visual stimuli.

Our study is the first complex, spatiotemporal analysis of visual cells in the extrageniculate visual pathway that employs a wide range of spatial and temporal frequencies and describes the particular spectral spatiotemporal filter properties of the collicular, suprageniculate and caudate visual neurons.

Our approach allows a direct comparison of the dynamic properties of these neurons with those in other areas of the brain. Table 1 lists the quantitative spatial and temporal visual properties of the subcortical and cortical visual regions investigated to date in the feline brain.

	Optimal spatial frequency (c/deg)	Spatial bandwidth (octaves)	Optimal temporal frequency (Hz)	Temporal bandwidth (octaves)
SC intermediate	0.06	1.06	9.06	2.07
SC superficial	0.10	1.84	6.84	2.38
CN	0.05	1.31	10.6	1.38
Sg	0.05	1.07	8.53	1.66
Lp-Pul	~0.20	2.20	~5.00	2.32
LGN X cells	0.85	-	2.50	-
LGN Y cells	0.14	-	5.20	-
LGN W cells	0.07	-	2.70	-
A17	0.90	1.50	2.90	1.70
A18	0.22	1.49	3.20	1.50
A19	0.17	1.90	3.00	2.90
A21a	0.27[2], 0.36[1]	1.60[1], 1.79[2]	3.25[2], 7.00[1]	1.92[2], 2.90[1]
A21b	0.08	2.20	3.20	3.30
PMLS	0.16	2.20	5.00	2.00
AES cortex	0.20	1.40	6.30	1.10

[1] *Tardif et al., 1996,*
[2] *Morley and Vickery, 1997*

Table 1. *Quantitative spatial and temporal visual properties of cortical and subcortical structures in the feline brain.*

The SC, Sg and CN visual cells clearly preferred drifting gratings with extremely low spatial frequencies: the mean optimal spatial frequency for the intermediate SC cells was 0.06 c/deg, for the Sg and CN cells it was 0.05 c/deg. This is comparable to that of the Y- and W-cells (possible source of visual inputs to the SC, the Sg and the CN)(Y-cells:Wang et al., 1998; 2001; W cells: Rowe et al., 1993) but much lower than that of the X-cells of the LGN (Saul and Humphrey, 1990; Humphrey and Murthy, 1999), the lateral posterior-pulvinar complex of the thalamus (Lp-Pul) (Casanova et al., 1989) and almost all striate and extrastriate cortical visual areas (Movshon et al., 1978b; Zumbroich and Blakemore, 1987; Tardif et al., 1996; 1997; Morley and Vickery, 1997; Bergeron et al., 1998; Nagy et al., 2003).

A majority of the collicular, suprageniculate and caudate visual units exhibited low-pass spatial tuning characteristics, though spatial band-pass and broad-band cells were also recorded. Low-pass cells are similarly common in the posteromedial lateral suprasylvian

(PMLS) area (Zumbroich and Blakemore, 1987), the anteromedial LS area (Ouellette et al., 2004), and the cortex along the anterior ectosylvian sulcus (AES cortex; Nagy et al., 2003a). Nevertheless, some low-pass tuned cells have also been observed in cortical areas 17 (Ikeda and Wright, 1975), 18 (Movshon et al., 1978b), 19 (Bergeron et al., 1998), 21a (Morley and Vickery, 1997; Tardif et al., 2000) and 21b (Tardif et al., 2000), the Lp-Pul and the LGN of the thalamus (see Saul and Humphrey, 1990, for X- and Y-cells; Humphrey and Murthy, 1999, for W-cell) and the W-cells of the retina (Rowe and Cox, 1993)

The band-pass SC, Sg and CN neurons are generally narrowly tuned to spatial frequencies. This might indicate that these cells could act as appropriate spatial filters. The spatial tuning width of the band-pass collicular, suprageniculate and caudate neurons is comparable not only with those of the the AES cortex (Nagy et al., 2003a) but also with that of the striate visual cortex (Movshon et al., 1978b), but smaller than those of the other visual regions of the feline brain (Tanaka et al., 1987; Zumbroich and Blakemore, 1987; Bergeron et al., 1998; Tardif et al., 2000; Ouelette et al., 2004; Waleszczyk et al., 2007).

All of the investigated extrageniculate visual neurons responded optimally to temporal frequencies ranged between 8.53 and 10.6 Hz. It is slightly higher than in the Lp-Pul (Casanova et al., 1989; Merabet et al., 1998), the AES cortex (Nagy et al., 2003a) and the LS areas (Morrone et al., 1986; Zumbroich and Blakemore, 1987; Ouellette et al., 2004), but much higher than those of areas 17 (Saul and Humphrey, 1992; Casanova, 1993), 18 (Saul and Humphrey, 1992), 19 (Bergeron et al., 1998), 21a (Morley and Vickery, 1997) and 21b (Tardif et al., 2000).

The temporal frequency tuning functions of these cells, similarly to those in the AES cortex (Nagy et al., 2003a) are mainly band-pass and rarely high-pass. The band-pass visual units in the tectal system displayed narrow temporal frequency tuning. This is comparable with the temporal tuning widths for the LS areas (Morrone et al., 1986), the AES cortex

(Nagy et al., 2003a), areas 17 and 18 (Movshon et al., 1978b), but much lower than those of the Lp-Pul (Casanova et al., 1989) and areas 19 (Bergeron et al., 1998), 21a (Tardif et al., 1996) and 21b (Tardif et al., 2000).

It is also worth to know that there is some degree of uncertainty about the pathways conveying sensory information to the CN. The concept of the corticostriatal pathways from the primary visual cortex was earlier widely accepted. Morphological findings on cats and rabbits demonstrated that the striate cortex sends sensory information to the CN (Webster, 1965; Hollander et al., 1979; Norita et al., 1991). However, more recent morphological and physiological studies support the role of the extrageniculate ascending tectofugal pathways to the CN in reptiles, birds and mammals (Harting et al., 2001a;b; McHaffie et al., 2001; Nagy et al., 2003b; 2005b; Guirado et al., 2005). The similar spatiotemporal visual properties - the preference for very low spatial and very high temporal frequencies and narrow spatial and temporal tuning- found in the SC, Sg and the CN also support the role of the extrageniculate tectal visual information toward the CN (Nagy et al., 2003b, 2008; Paróczy et al., 2006; Waleszczyk et al., 2007). The dorsolateral aspect of the caudate body in the cat can receive its visual afferentation from the tectum via the Sg of the posterior thalamus (Harting et al., 2001a; Nagy et al., 2003). It must be mentioned here that the primary visual cortex has spatial and temporal tuning widths that are slightly larger than, though still comparable (Movshon et al., 1978a) with those of the CN. However, this is as far as the similarity goes between the spectral spatiotemporal properties of the CN and area 17. Spatial low-pass units are rare in area 17, but most common in the extrageniculate subcortical and extrastriate cortical regions (Pinter and Harris, 1981; Casanova et al., 1989; Nagy et al., 2003; Paróczy et al., 2006; Waleszczyk et al., 2007). Further, the optimal spatial and temporal frequency preferences of the CN units are considerably different from those in area 17 (Movshon et al., 1978b). This suggests that the CN neurons receive strong Y- or W-

signals probably from the SC, via the Sg of the thalamus and also from the AES cortex (Benedek et al., 1996; Nagy et al., 2003a; 2005; 2008; Eördegh et al., 2005; Paróczy et al., 2006) and tends to discount high spatial and low temporal frequency X-input from area 17 (Movshon et al., 1978b).

7. Conclusions

The neurons in the intermediate and deep layers of the SC, the Sg and the CN possess very similar visual receptive field properties. These strong similarities suggest their common role in visual information processing and the connected visuomotor processes. It has been reported earlier that all motion detectors are apparently finely tuned to temporal and spatial frequencies (Anderson and Burr, 1985), the narrow tuning aiding the velocity detection and the analysis of the object in motion (Burr and Ross, 1986; Burr et al., 1986). The neurons with their large receptive fields, with their preferences for low spatial frequencies and with their fine spatial and temporal tuning, have all the capacities required to perceive optic flow, i.e. they are good candidates for tasks involved in the perception of self-motion (Morrone et al., 1986; Brosseau-Lachaine et al., 2001). These properties enable the feline extrastriatal visual system to play an important role in the recording of movements of the visual environment relative to the body, and in helping its participation in the adjustment of motor behavior to environmental challenges.

8. Summary

Electrophysiological recordings of single units in the intermediate layers of the SC, in the Sg and the CN were carried out extracellularly via tungsten microelectrodes in halothane-anesthetized, immobilized, artificially respirated cats. Neuronal activities were recorded and correlated with the movement of the light stimulus by a computer and stored for further analysis as PSTHs. The net firing rate was calculated as the difference between the firing rates during the prestimulus and peristimulus intervals. The net firing rate was defined as a response when a t-test revealed a significant ($p<0.05$) difference between the two values. Vertical penetrations were performed between the Horsley-Clarke co-ordinates anterior 6 to posterior 1, lateral 0-6 in the stereotaxic depths in the interval 15-17 to record SC; anterior 4.5-6.5, lateral: 4-6.5 in the stereotaxic depths in the interval 16-18 to record Sg; anterior 12-17 and lateral 4-6.5 in the stereotaxic depths in the interval 12-19 to record CN neurons.

The visual receptive field properties and spatiotemporal freuqency tuning function of altogether 99 visually responsive single-units in the intermedate layers of the SC, 105 in the Sg and 101 in the CN were analyzed in details.

Subjective estimation of the extents of the visual receptive fields were performed by listening to the neuronal responses to the movements of a light spot generated by a handheld lamp. Our subjective estimation indicated that the visual receptive fields were extremely large (consistently larger than 6000 deg^2) in case of the Sg and the CN: they covered a major part of the contralateral hemifield and extended deep into the ipsilateral one, yielding a receptive field that overlapped almost totally with the visual field of the right eye. The receptive fields consistently included the area centralis. No signs of retinotopical organization were observed within the Sg of the posterior thalamus or in the CN. Neurons in the intermediate and deep layers of the SC similarly display large receptive fields that often

extend into the ipsilateral hemifield (Wallace et al., 1998).The mean size of the receptive fields in the intermediate SC was 1890.69 degree^2.

The direction sensitivity and tuning functions of the neurons in the intermediate SC layers, the Sg and the CN were determined on the basis of their responses to the drifting sinusoidal gratings moving in 8 different directions (4 different axes of movement). The preferred directions varied considerably in the cells recorded. A majority of the cells in the SC and the CN exhibited broad directional tuning and were non-direction selective. The suprageniculate visually active neurons displayed narrow directional tuning and high direction selectivity.

The most noteworthy findings of this work are that we described and compared the spatial and temporal visual receptive field properties of the single-neurons along the tecto-thalamo-basal ganglia pathway. The SC, Sg and CN visual cells were strongly selective to low spatial frequencies: the mean optimal spatial frequency for the intermediate SC cells was 0.06 c/deg (N=99, SD: ±0.02 c/deg, Range: 0.025-0.25 c/deg), for the Sg and CN cells they were 0.05 c/deg (Sg: N=105, SD±0.04 c/deg, Range: 0.02-0.2 c/deg ; CN: N=89, SD: ±0.03 c/deg, Range: 0.025-0.18 c/deg). Most of the collicular, suprageniculate and caudate visual units exhibited low-pass spatial tuning characteristics, though spatial band-pass and broad-band cells were also recorded. The band-pass SC, Sg and CN neurons were generally narrowly tuned to spatial frequencies. All of the investigated extrageniculate visual neurons responded optimally to high temporal frequencies. The optimal temporal frequencies of the intermediate SC (N=99, mean: 9.06±5.49 Hz, Range: 1.71-31.19 Hz), Sg (N=105, mean: 8.53±4.43 Hz, Range: 0.07-26.41 Hz) and CN (N=89, mean: 10.6±4.8 Hz, Range: 4.6-27.6 Hz) visually active neurons were observed in the range between 8.53 and 10.6 Hz. The temporal frequency tuning functions of these cells were mainly band-pass and rarely high-pass. The band-pass visual units in the tecto-thalamo-CN system displayed narrow temporal frequency tuning.

Our results suggest that the extrageniculate neurons are the most narrowly tuned visual units to temporal frequencies in the feline brain. This fine spatial and temporal tuning characteristic of the intermediate SC, Sg and CN neurons suggests that they are good spatial and temporal filters. They respond optimally to moving visual stimuli; their responsivity to stationary stimulation is much lower. These neurons seem to be novelty detectors. Our results that describe the spatio-temporal visual characteristics of the tecto-thalamo-basal ganglia pathway suggest a special behavioral role of this visual system. The narrowly spatial and temporal tuning aids the velocity detection and the analysis of the object in motion. The extrageniculate visual system may be involved in the optic flow processing and could be a good candidate for tasks involved in the perception of self-motion. We suggest that the intermediate SC, Sg and CN neurons may play a role in the recording of movements of the visual environment relative to the body and thus they may participate in the adjustment of motor behavior in response to environmental challenges.

In summary, our results add new data concerning the visual representation of the environment in the mammalian brain and may help to clarify the functional role of the extrageniculate system in visual (multisensory) processing and the connected behavioural actions.

9. Acknowledgements

I respectfully thank Professor György Benedek who has served as my mentor and supervisor and for the opportunity that I could work with him. I greatly appreciate his helpful and instructive guidance. I express my gratitude to Professor Gábor Jancsó for allowing me to work in the Neuroscience PhD Program. I wish to express my deepest thanks to Dr. Attila Nagy for his generously help and support during my scientific work. My special thanks go to Dr. Zita Márkus, Dr. Antal Berényi and Dr. Alice Rokszin for their help and friendship. I would like to acknowledge the help of Gábor Braunitzer, Péter Gombkötő, Ágnes Farkas and Andrea Pető.

I express my most sincere gratitude to Gabriella Dósai for her valuable technical assistance and for the preparation of high-quality figures for my thesis. Many thanks are due to Péter Liszli for his expert help in solving hardware and software problems.

I would like to express my thanks to all colleagues in the Department of Physiology for their support and kindness. It was good to work with them in this department.

My deepest thanks are due to my family for their continuous love and help in my life.

Our experiments were supported by OTKA/Hungary grant F048396, OTKA/Hungary grant 42610 and FKFP/Hungary grant 0455/2000.

10. List of abbreviations

AES: anterior ectosylvian sulcus

AEV: anterior ectosylvian visual area

CN: caudate nucleus

CSF: contrast sensitivity function

DI: direction selectivity index

LGN: lateral geniculate nucleus

LGNd: dorsal lateral geniculate nucleus

LM-Sg: lateralis-medialis suprageniculate nucleus

Lp-Pul: lateral posterior-pulvinar complex

PMLS: posterior-medial devision of the lateral suprasylvian area

PSTH: peristimulus time histogram

SC: superior colliculus

SN: substantia nigra

11. References

Anderson SJ, Burr DC (1985) Spatial and temporal selectivity of the human motion detection system. *Vision Res 25:1147-1154.*

Barlow HB (1972) Book Review. *Vision Res 13(2): 525.*

Benedek G, Fischer-Szatmári L, Kovács G, Perényi J, Katoh YY (1996) Visual, somatosensory and auditory modality properties along the feline suprageniculate-anterior ectosylvian sulcus/insular pathway. *Prog Brain Res 112:325-334.*

Benedek G, Perényi J, Kovács G, Fischer-Szatmári L, Katoh YY (1997) Visual, somatosensory, auditory and nociceptive modality properties in the feline suprageniculate nucleus. *Neuroscience 78:179-189.*

Bergeron A, Tardif E, Lepore F, Guillemot JP (1998) Spatial and temporal matching of receptive Weld properties of binocular cells in area 19 of the cat. *Neuroscience 86:121–134.*

Bishop PO, Kozak W, Vakkur GJ (1962) Some quantitative aspects of the cat's eye: axis and plane of reference, visual field coordinates and optics. *J Physiol 163:466–502.*

Blakemore c, Campbell FW (1969) On the existence of neurones in the human visual system selectively sensitive to the orientation and size of retinal images. *J Physiol 203: 237-260.*

Blakemore C, Sutton P (1969) Size adaptation: a new aftereffect. *Science 166(902):245-7.*

Brosseau-Lachaine O, Faubert J, Casanova C (2001) Functional sub-regions for optic flow processing in the posteromedial lateral suprasylvian cortex of the cat. *Cereb Cortex 11:989-1001.*

Burke W, Dreher B, Wang C (1998) Selective block of conduction in Y optic nerve fibres: significance for the concept of parallel processing. *Eur J Neurosci 10: 8-19.*

Burr DC, Ross J (1986) Visual processing of motion. *Trends Neurosci 9:304-307.*

Burr DC, Ross J, Morrone M (1986) Seeing objects in motion. *Proc Roy Soc Lond B227:249-265.*

Campbell FW, Robson JG (1968) Application of Fourier analysis to the visibility of gratings. *J. Physiol. 197: 551-566.*

Campbell FW, Maffei L, Piccolino M (1973) The contrast sensitivity of the cat. *J Physiol. 229(3):719-31.*

Casanova C, Freeman RD, Nordmann JP (1989) Monocular and binocular response properties of cells in the striate-recipient zone of the cat's lateral posterior-pulvinar complex. *J Neurophysiol 62:544-557.*

Casanova C (1993) Response properties of neurons in area 17 projecting to the striate-recipient zone of the cat's lateralis posterior-pulvinar complex: comparison with cortico-tectal cells. *Exp Brain Res. 1993;96(2):247-59.*

Dec K, Waleszczyk WJ, Wróbel A, Harutiunian-Kozak BA (2001) The spatial substructure of visual receptive Welds in the cat’s superior colliculus. *Arch Ital Biol 139:337–355.*

De Valois RL, De Valois EW (1988) Spatial vision. *New York: Oxford University Press.*

Dreher B, Sanderson KJ (1973) Receptive field analysis: responses to moving visual contours by single lateral geniculate neurones in the cat. *J Physiol 234: 95-118.*

Dreher B, Michalski A, Ho RTH, Lee CWF, BurkeW (1993) Processing form and motion in area 21a of cat visual cortex. *Vis Neurosci 10: 93-115.*

Dreher B, Wang C, Burke W (1996) Limits of parallel processing: excitatory convergence of different information channels on single neurons in striate and extrastriate visual cortices. *Clin Exp Pharmacol Physiol 23: 913-925.*

Eördegh G, Nagy A, Berényi A, Benedek G (2005) Processing of spatial visual information along the pathway between the suprageniculate nucleus and the anterior ectosylvian cortex. *Brain Res Bull 30;67(4):281-9.*

Guirado S, Real MA, Davila JC (2005) The ascending tectofugal visual system in amniotes: new insights. *Brain Res Bull 66:290-296.*

Harting JK, Updyke BV, Van Lieshout DP (1992) Corticotectal projections in the cat: anterograde transport studies of twenty-five cortical areas. *J Comp Neurol 324:379-414.*

Harting JK, Updyke BV, Van Lieshout DP (2001a) Striatal projections from the cat visual thalamus. *Eur J Neurosci 14:893-896.*

Harting JK, Updyke BV, Van Lieshout DP (2001b) The visual-oculomotor striatum of the cat: functional relationship to the superior colliculus. *Exp Brain Res 136:138-142.*

Hashemi-Nezhad M, Wang C, Burke W, Dreher B (2003) Area 21a of cat visual cortex strongly modulates neuronal activities in the superior colliculus. *J Physiol (Lond) 550:535–552.*

Hikosaka O, Sakamoto M, Usui S (1989) Functional properties of monkey caudate neurons. II. Visual and auditory responses. *J Neurophysiol 61:799-813.*

Hollander H, Tietze J, Distel H (1979) An autoradiographic study of the subcortical projections of the rabbit striate cortex in the adult and during postnatal development. *J Comp Neurol 184:783-794.*

Holub RA, Morton-Gibson M (1981) Response of visual cortical neurones of the cat to moving sinusoidal gratings : Response contrast functions and spatiotemporal interactions. *J. Neurophysiol. 46: 1244-1259.*

Hoshino K, Nagy A, Eördegh G, Benedek G, Norita M. (2004) Two types of neuron are found within the PPT, a small percentage of which project to both the LM-SG and SC. *Exp Brain Res. 155(4):421-6.*

Hubel DH, Wiesel TN (1962) Receptive fields, binocular interaction and functional architecture in the cat's visual cortex. *J Physiol 160:106-154.*

Hubel DH, Wiesel TN (1977) Ferrier lecture. Functional architecture of macaque monkey visual cortex. *Proc R Soc Lond B Biol Sci. 1977 Jul 28;198(1130):1-59.*

Humphrey AL, Murthy A (1999) Cell types and response timings in the medial interlaminar nucleus and C-layers of the cat lateral geniculate nucleus. *Vis Neurosci 16:513-525.*

Ikeda H, Wright MJ .(1975) Spatial and temporal properties of "sustained" and "transient" neurones in area 17 of the cat's visual cortex. *J Physiol 22:363-383.*

Lee BB, Willshaw DJ (1978) Responses of the various types of cat retinal ganglion cells to moving contours. *Vision Res 18: 757-765.*

Livingstone MS, Hubel DH (1988) Segregation of form, color, movement, and depth: anatomy, physiology, and perception. *Science 240: 740-749.*

McHaffie JG, Thomson CM, Stein BE (2001) Corticotectal and corticostriatal projections from the frontal eye fields of the cat: an anatomical examination using WGA-HRP. *Somatosens Mot Res18 :117-130.*

McIlwain JT, Lufkin RB (1978) Distribution of direct Y-cell inputs to the cat’s superior colliculus: are there spatial gradients? *Brain Res 103: 133-138.*

McLean J, Palmer LA (1989) Responses of simple cells in areas 17 and 18 of the cat in the spatiotemporal frequency domain. *Inv. Opt. Vis. Sci. 30: 111.*

Mendola JD, Payne BR (1993) Direction selectivity and physiological compensation in the superior colliculus following removal of areas 17 and 18. *Vis Neurosci 10:1019–1026.*

Merabet L, Desautels A, Minville K, Casanova C (1998) Motion integration in a thalamic visual nucleus. *Nature 396:265-268.*

Morley JW, Vickery RM (1997) Spatial and temporal frequency selectivity of cells in area 21a of the cat. *J Physiol (Lond) 501:405–413.*

Morrone MC, Di Stefano M, Burr DC (1986) Spatial and temporal properties of neurons of the lateral suprasylvian cortex of the cat. *J Neurophysiol 56:969-986.*

Movshon JA, Thompson ID, Tolhurst DJ (1978a) Spatial summation in the receptive fields of simple cells in the cat's striate cortex. *J Physiol (Lond) 283: 53-77.*

Movshon JA, Thompson ID, Tolhurst DJ (1978b) Spatial and temporal contrast sensitivity of neurones in areas 17 and 18 of the cat's visual cortex. *J Physiol (Lond) 283:101–120*

Nagy A, Eördegh G, Benedek G (2003a) Spatial and temporal visual properties of single neurons in the feline anterior ectosylvian visual area. *Exp Brain Res 151:108-114.*

Nagy A, Eördegh G, Norita M, Benedek G (2003b) Visual receptive field properties of neurons in the feline caudate nucleus. *Eur J Neurosci 18:449-452.*

Nagy A, Eördegh G, Norita M, Benedek G (2005a) Visual receptive field properties of excitatory neurons in the substantia nigra. *Neuroscience 130:513-518.*

Nagy A, Paróczy Z, Norita M, Benedek G (2005b) Multisensory responses and receptive field properties of neurons in the substantia nigra and in the caudate nucleus. *Eur J Neurosci 22:419-424.*

Nagy A, Paróczy Z, Márkus Z, Berényi A, Wypych M, Waleszczyk WJ, Benedek G

(2008) Drifting grating stimulation reveals particular activation properties of visual neurons in the caudate nucleus. *Eur J Neurosci27(7):1801-8.*

Norita M, Mucke L, Benedek G, Albowitz B, Katoh YY, Creutzfeldt OD (1986) Connections of the anterior ectosylvian visual area (AEV). *Exp Brain Res 62:225-240.*

Norita M, Hicks TP, Benedek G, Katoh YY (1991) Organization of cortical and subcortical projections to the feline insular visual area, IVA. *J Hirnforsch 32:119-134.*

Paróczy, Z., Nagy, A., Márkus, Z., Waleszczyk, W.J., Wypych, M. & Benedek, G. (2006) Spatial and temporal visual properties of single neurons in the suprageniculate nucleus of the thalamus. *Neuroscience, 137, 1397-1404.*

Pasternak T (1986) The role of cortical directional selectivity in detection of motion and flicker. *Vision Res. 26(8):1187-94.*

Pettigrew JD, Cooper ML, Blasdel GG (1979) Improved use of tapetal reflection for eye-position monitoring. *Invest Ophthalmol Vis Sci 18:490–495.*

Pinter RB, Harris LR (1981) Temporal and spatial response characteristics of the cat superior colliculus. *Brain Res 207:73-94.*

Pouderoux C, Freton E (1979) Patterns of unit responses to visual stimuli in the cat caudate nucleus under chloralose anesthesia. *Neurosci Lett 11:53-58.*

Ouellette BG, Minville K, Faubert J, Casanova C (2004) Simple and complex visual motion response properties in the anterior medial bank of the lateral suprasylvian cortex. *Neuroscience 123:231–245.*

Robson JG (1966) spatial and temporal contrast sensitivity functions of the visual system. *J. opt. Soc. Am. 56: 1141-1142.*

Rosenquist AC (1985) Cerebral Cortex Volume 3 Visual Cortex. Peters A, Jones EG editors Connenctions of visual Cortical Areas in the Cat. New York, *Plenum Press 81-117.*

Rowe MH (1991) Functional organization of the retina. In: Neuroanatomy of the visual pathways and their development, (Eds. B. Dreher and S.R. Robinson), *Vision and Visual Dysfunction, Vol. 4 (series ed. J. Cronly-Dillon) Macmillan, London, p. 1-68.*

Rowe MH, Cox JF (1993) Spatial receptive-field structure of cat retinal W cells. *Vis Neurosci 10:765-79.*

Sanderson KJ (1971) The projection of the visual field to the lateral geniculate and medial interlaminar nuclei in the cat. *J Comp Neurol 143:101-108.*

Saul AB, Humphrey AL (1990) Spatial and temporal response properties of lagged and nonlagged cells in cat lateral geniculate nucleus. *J Neurophysiol 64:206-224*.

Saul AB, Humphrey AL (1992) Temporal-frequency tuning of direction selectivity in cat visual cortex. *Vis Neurosci. 1992 Apr;8(4):365-72*.

Schade OH Sr (1956) Optical and photoelectric analog of the eye. J. *opt. Soc. Am. 46:721-739.*

Sireteanu R, Hoffmann KP (1979) Relative frequency and visual resolution of X- and Y-cells in the LGN of normal and monocularly deprived cats: interlaminar differences. *Exp Brain Res 34: 591-603.*

Stein BE, Meredith MA (1991) Functional organization of the superior colliculus. Leventhal AG (ed) The neural basis of visual function. In: *Cronly-Dillon J (series ed) Vision and visual dysfunction, vol 4, Macmillan, London, pp 85–110.*

Stone J (1983) Parallel processing in the visual system. *Plenum Press, New York, 438 p.*

Stone J, Hoffmann KP (1972) Very slow-conducting ganglion cells in the cat's retina: a major, new functional type? *Brain Res 43: 610-616.*

Stone J, Dreher B, Leventhal A (1979) Hierarchical and parallel mechanisms in the organization of visual cortex. *Brain Res 180: 345-94.*

Sur M, Sherman SM (1982) Linear and nonlinear W-cells in C-laminae of the cat's lateral geniculate nucleus. *J Neurophysiol 47: 869-884.*

Tanaka K, Ohzawa I, Ramoa AS, Freeman RD (1987) Receptive field properties of cells in area 19 of the cat. *Exp Brain Res 65:549-558.*

Tardif E, Bergeron A, Lepore F, Guillemot JP (1996) Spatial and temporal frequency tuning and contrast sensitivity of single neurons in area 21a of the cat. *Brain Res 716:219–223.*

Tardif E, Richer L, Bergeron A, Lepore F, Guillemot JP (1997) Spatial resolution and contrast sensitivity of single neurons in area 19 of split-chiasm cats: a comparison with primary visual cortex. *Eur J Neurosci 9:1929–1939.*

Tardif E, Lepore F, Guillemot JP (2000) Spatial properties and direction selectivity of single neurons in area 21b of the cat. *Neuroscience 97:625–634.*

Tolhurst DJ (1973) Separate channels for the analysis of the shape and the movement of moving visual stimulus. *J Physiol. 231(3):385-402.*

Tolhurst DJ, Movshon JA (1975) Spatial and temporal contrast sensitivity of striate cortical neurones. *Nature Lond. 257: 674-675.*

Waleszczyk WJ, Wang C, Burke W, Dreher B (1999) Velocity response profiles of collicular neurons: parallel and convergent visual information channels. *Neuroscience 93:1063–1076.*

Waleszczyk WJ, Nagy A, Wypych M, Berényi A, Paróczy Z, Eördegh G, Ghazaryan A, Benedek G (2007) Spectral receptive field properties of neurons in the feline superior colliculus. *Exp Brain Res. 2007 Jul;181(1):87-98.*

Wallace MT, Meredith MA, Stein BE (1998) Multisensory integration in the superior colliculus of the alert cat. *J Neurophysiol 80:1006-1010*.

Wang C, Dreher B, Assaad N, Ptito M, Burke W (1998) Excitatory convergence of Y and non-Y channels onto single neurons in the anterior ectosylvian visual area of the cat. *Eur J Neurosci 10:2945-2956.*

Wang C, Waleszczyk WJ, Benedek G, Burke W, Dreher B (2001) Convergence of Y and non-Y channels onto single neurons in the superior colliculi of the cat. *Neuroreport 12:2927-2933.*

Webster KE (1965) The cortico-striatal projections in the cat. *J Anat 99:329-337*.

Zumbroich TJ, Blakemore C (1987) Spatial and temporal selectivity in the suprasylvian visual cortex of the cat. *J Neurosci 7:482–500.*

Zumbroich T, Price DJ, Blakemore C (1988) Development of spatial and temporal selectivity in the suprasylvian visual cortex of the cat. *J Neurosci. 8(8):2713-28.*